Time-temperature equivalence in environmental stress cracking of high-density polyethylene

Marco Contino*, Luca Andena, Marta Rink
Dipartimento di Chimica, Materiali e Ingegneria Chimica "G.Natta", Politecnico di Milano, Piazza Leonardo da Vinci 32, 20133 Milano, Italy

Giuliano Marra, Stefano Resta
Fater S.p.A., R&D division, Via Ardeatina 100, 00071 Pomezia, Italy

*Corresponding author. Tel.: +390223993210;
 E-mail address: marco.contino@polimi.it

This paper is dedicated to Francesco Caimmi, our colleague and friend who left us at an early age in September 2017 and whose memory accompanies us daily.

Abstract

In this work the environmental stress cracking resistance of two high-density polyethylene grades, employed for the manufacturing of bleach bottles, was investigated by using a fracture mechanics approach. Two aqueous solutions similar to common bleach products (with and without sodium hypochlorite) were considered as the active environment, whose effect on both the initiation and propagation phases of fracture was evaluated for the two materials. Tests at different temperatures were performed and a time-temperature superposition scheme was applied both in air and in the active environment. Temperature was shown to influence fracture behaviour only through the material inherent viscoelasticity.

Keywords

ESC, time-temperature superposition, Fracture mechanics, HDPE

Nomenclature

a	Crack length
$\dot{a}$	Crack speed
$\dot{a}^*$	Critical crack speed
$a_T^{T_0}$	Shift factor
B	Specimen thickness
B_g	Thickness of the grooved section of the specimen
K	Stress intensity factor
K_i	Stress intensity factor of the specimen i
$\widehat{K}_i$	Value of the interpolating function for the specimen i
K_i^*	Critical stress intensity factor in initiation
K_p^*	Critical stress intensity factor in propagation
S	Span
s_ε	Standard deviation
t_i	Initiation time
$t_{i,i}$	Initiation time of the specimen i
$\bar{t}_i$	Average crack initiation time
t_i^*	Critical interaction time
m	Slope
n	Number of experimental data
P	Load
q	Intercept
T	Temperature
T_0	Reference temperature
W	Specimen width
Y	Shape factor
$\varepsilon(m)$	Standard error related to the slope
$\varepsilon(q)$	Standard error related to the intercept
$\varepsilon_T^{T_0}$	Standard error related to the determination of the shift factor

1 Introduction

High-density polyethylene (HDPE) is a polymer used for many packaging applications. During service life, the material can be exposed to substances, like household detergents, that can affect its mechanical behaviour. Environmental Stress Cracking (ESC) may occur in polymers through the combined action of mechanical stress and active chemicals. ESC is related to local plasticization, craze/crack initiation and its/their propagation and it can lead to the premature failure of the component [1- 6].

The ESC phenomenon shares many aspects with slow crack growth naturally occurring in polymers continuously subjected to mechanical stress [7], as in the case of pressurized pipes; the evolution in time of the fracture process is caused by the material viscoelasticity. The lifetime of a given product is thus determined by the sum of the initiation time, required for a crack to start growing, and the propagation time, needed for the crack to advance through the component thickness. In the presence of some substances these phenomena occur faster and, in fact, known ESC agents such as detergents are commonly used to accelerate testing on pipe materials [8-10].

Fracture mechanics has been successfully applied to the study of fracture in viscoelastic materials, as reported in several instances in the existing scientific literature [11-14]. Its use has been extended directly to study ESC of several systems [15, 16], including: polystyrene in oil [17-19], polyethylene in various detergents [20-22] and polyethyleneterephtalate in sodium hydroxide [23].

The specific case of HDPE in bleach had already been addressed in a previous study by the authors [24], in which the ESC resistance of two blow-moulding HDPE grades, employed in the manufacturing of bleach bottles, was investigated by using fracture mechanics. In this work only fracture initiation had been considered and tests were conducted at 60°C to accelerate the fracture phenomenon. As confirmed by preliminary chemical interaction studies [24], it has to be remarked that the pH-stabilized commercial bleach solutions employed in this study have negligible active chlorine content and thus limiting oxidizing effects on the bulk material.

The focus of the present investigation was to extend the previous study with the aim of making reliable predictions of the material behaviour under service life conditions. For this purpose, the investigation also includes the propagation stage following crack initiation. More importantly, tests at different temperatures were performed in view of quantifying the accelerating effect that temperature has on fracture behaviour, thus allowing service life predictions at room temperature to be made. For this purpose, the applicability of a time-temperature superposition scheme was evaluated and the relevant initiation and propagation master curves were obtained; to the authors knowledge, this has never been attempted in conjunction with a fracture-mechanics based description of ESC.

This approach represents a valuable engineering tool for the prediction of ESCR of polymeric components.

2 Materials and methods

2.1 Experimental details

Two blow-moulding HDPE grades, reported as having nominally different molecular weight distributions (MWD), were supplied in pellet form by FATER S.p.A.. Although quantitative MWDs are not available, they are known to possess monomodal and bimodal ones, with the

bimodal having a significant larger amount of long polymeric chains. In the following they will be referred to as HDPE-MONO and HDPE-BI, respectively.

11 mm thick plates were manufactured via compression moulding using the following procedure:

- the mould was heated to 190°C
- HDPE pellets were put into the mould for 5 minutes without pressure
- a pressure of about 20 bar was applied for 5 minutes
- a pressure of about 40 bar was applied for 5 minutes
- the mould was cooled down to room temperature with a water cooling system

Plates were subsequently thermally treated at 130°C for 40 minutes in order to reduce thermal stresses in the material and avoid distortions in the final samples. After moulding, the two materials showed a very similar degree of crystallinity (70%), as measured by differential scanning calorimetry.

Single Edge Notched Bending (SENB) specimens having dimensions shown in Figure 1 were obtained from the plates via circular saw cutting and subsequent milling. A V-profile groove was introduced, with a milling machine, along the notch plane on both sides of the specimens, to guide crack propagation. Notches were made via automated "chisel-wise" cutting with a sharp blade, obtaining a final notch root radius lower than 10 µm. A series of SENB blunt notched samples was also prepared using a circular profile blade with 1 mm radius; these specimens were used in creep testing for the compliance calibration used to detect crack initiation, as described later.

From five up to more than twenty samples were tested at five different temperatures (23, 31, 40, 50 and 60°C), applying two different loading histories: constant displacement rate (from 0.001 up to 200 mm/min) and various constant loads (creep) adopting three- and four-point bending configurations, respectively (see Figure 1). These two loading histories allowed the exploration of different time ranges, with shorter and longer tests performed on a universal testing machine and dedicated custom-built ones, respectively. Previous works on polyethylene [21, 24] and high-impact polystyrene [17] clearly showed that obtained results were independent on the applied loading history and testing configuration.
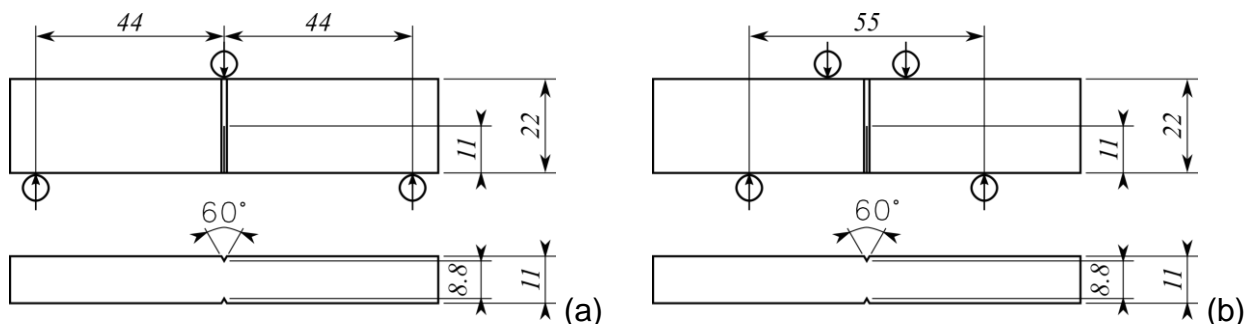

Figure 1 - Specimen geometries and nominal dimensions (in mm). (a) SENB in three point bending for constant displacement rate tests; (b) SENB in four point bending configuration for constant load (creep) tests.

Fracture tests were first conducted to obtain the reference fracture behaviour in air. Subsequently the effect of the active environment was investigated by testing specimens placed in flexible polyethylene bags filled with two different solutions:

- Sol. A: an aqueous solution of sodium hypochlorite, sodium hydroxide, sodium carbonate, surfactants and perfume;
- Sol. B: a similar solution, in which sodium hypochlorite was replaced with water

Sol. A has a composition identical to commonly employed household bleach while the purpose of testing Sol. B was to verify whether the main component of commercial bleach (sodium hypochlorite) has an effect on ESC.

Constant displacement rate tests were performed on an Instron 1185R5800 electro-mechanical dynamometer equipped with a 10 kN load cell measuring the sample deflection directly from the crosshead displacement. Crack initiation and propagation were monitored using a 10 MPixel uEye UI 5490 SE camera. Nevertheless, the formation of rim films near the crack tip during the tests prevented in most cases a reliable determination of crack initiation by visual means (see Figure 2). In those instances in which optical detection could be performed, crack initiation was found to occur very close to the maximum of the load-time curve; the latter was therefore taken as a more objective criterion to identify crack initiation. Due to the rim films persistence also during crack growth, it was not possible to obtain any information regarding the propagation behaviour of the two materials subjected to this loading history.
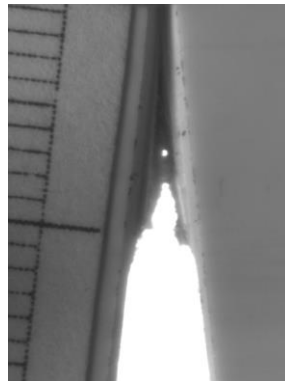
Figure 2 – Example of a video frame recorded during a fracture test. The formation and evolution of the rim film prevents visual determination of crack length with sufficient accuracy.

Creep tests were conducted on a custom-built testing machine featuring two fixed lower pins and two top ones on which the load was applied by means of a pneumatic device, able to release a dead weight in a controlled way within a few seconds. Specimen deflection at the load pins was measured by a Linear Variable Displacement Transducer (LVDT). The design of these testing machines is such that visual observation of the crack is not possible. To measure crack length a method similar to the one adopted in [17], was used. To apply this procedure it is necessary to determine the compliance of specimens with blunt notches, subjected to the same loading conditions used for the actual fracture tests: in absence of a sharp notch, crack initiation does not occur within the timeframe of practical interest. From this information, and from the compliance of the specimens with sharp notches during the fracture tests it was possible to determine the crack length at any time during any given fracture test.

2.2 Fracture data analysis

The material behaviour in terms of both crack initiation and propagation can be represented by characteristic curves which relate the applied stress intensity factor, K, to initiation time, t_i, and crack speed, $\dot{a}$, respectively. In this work the fracture behaviour was analysed according to linear elastic fracture mechanics (LEFM). LEFM applicability for the two HDPEs under study had already been evaluated in [24], with the investigation of relevant size effects. It was found that, with a proper choice of specimen dimensions, K can be taken as a valid fracture parameter.

2.2.1 Constant displacement rate tests

For samples tested in three-point bending configuration, the stress intensity factor K was calculated according to [25]:

$$K = Y \frac{P}{B_g \sqrt{W}} \qquad (1)$$

In Equation 1 P is the applied load, W and B_g are the specimen width and the thickness of its grooved section, respectively, and Y is the relevant shape factor as given by Equation 2:

$$Y = \frac{3 \frac{S}{W} \sqrt{\frac{a}{W}}}{2 \left(1 + 2\frac{a}{W}\right)\left(1 - \frac{a}{W}\right)^{3/2}} \left\{1.99 - \frac{a}{W}\left(1 - \frac{a}{W}\right)\left[2.15 - 3.93\frac{a}{W} + 2.7\left(\frac{a}{W}\right)^2\right]\right\} \qquad (2)$$

in which S is the span between the lower pins and a is the crack length. As reported in the previous section, crack initiation was considered to occur at the maximum of the load-time curve.

2.2.2 Creep tests

For samples tested in four point bending, K was evaluated according to the expression for SENB specimens in pure bending, proposed in [26]:

$$K = Y \frac{PS\sqrt{\pi a}}{B^* W^2} \qquad (3)$$

The shape factor Y, which is valid up to $\frac{a}{W} = 0.6$, can be evaluated according to Equation 4:

$$Y = 1.12 - 1.39\left(\frac{a}{W}\right) + 7.32\left(\frac{a}{W}\right)^2 - 13.1\left(\frac{a}{W}\right)^3 + 14.0\left(\frac{a}{W}\right)^4 \qquad (4)$$

An effective thickness, B^*, was considered in Equation 3 to take into account the effect of the side grooves on the stress distribution in the specimen ligament. As reported in [17], for the four point bending samples B^* can be evaluated according to Equation 5:

$$B^* = B^{0.263} B_g^{0.737} \qquad (5)$$

with B being the nominal (i.e. ungrooved) sample thickness.

To identify the initiation time and crack growth speed a procedure based on compliance calibration, already reported in detail in [17, 20, 24], was adopted. The method is based on the separation of the contributions of the material viscoelasticity and crack propagation to the time-dependent portion of the specimen compliance, C, obtained from the displacements measured experimentally by the LVDT. As reported in Figure 3 for HDPE-MONO at 60°C and with initial applied K of 0.5 MPa·m$^{1/2}$, the material creep behaviour was characterized by performing tests on blunt notched samples, in which crack initiation did not occur. By comparing the compliance of sharp-notched samples with this reference behaviour, crack initiation could be detected when the difference between the two exceeded a pre-set tolerance of 1%. In the following, current crack length was determined at any time during a given test, thus allowing for monitoring of crack propagation speed. Because of significant data scatter due to irregular crack propagation when rim filming occurred, only a single average value of crack speed was computed for each specimen in the validity range of Y ($0.5 < \frac{a}{W} < 0.6$).
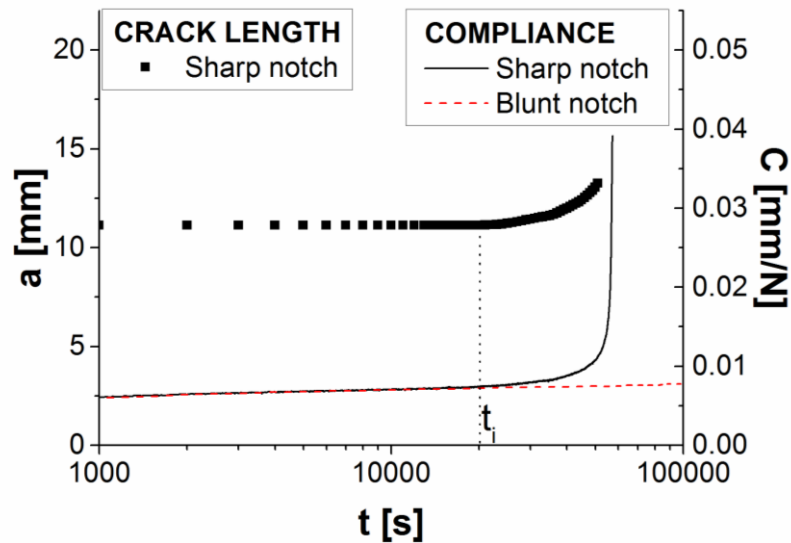
Figure 3 - Sample compliance-time curves for HDPE-MONO at 60°C and an initial applied stress intensity factor of 0.5 MPa·m1/2. Crack length can be determined by comparing the compliance of blunt and sharp notched samples as reported in [17].

2.3 Time-temperature superposition

If the time-temperature equivalence postulate applies for a given viscoelastic function (typically modulus or compliance), curves as a function of time obtained for a given material at different temperatures can be superimposed to give a so-called *master curve*. The rationale behind this is that the same physical phenomena occur within a broad temperature range, within which the effect of temperature is only to alter the time-scale of these phenomena. This scaling factor coincides with a translation (in log-scale of time) of the same viscoelastic function for the different temperatures considered.

This well-known approach had already been successfully applied not only at small strains but also to yield and fracture of polymers [11, 27-30]. Yet, its application in presence of an aggressive environment could not be taken for granted: in principle, temperature could have an effect on the activity or diffusion of the specific ESC agent, which would combine with the intrinsic temperature dependence expected from viscoelasticity alone. Verification of the applicability of the time-temperature equivalence in this case was the main aim of the present work.

2.3.1 Shift factor determination

In order to determine the shift factor required to superimpose the curves obtained at different temperatures, and to estimate the associated error, the following procedure, qualitatively sketched in Figure 4 for initiation in air, was adopted.
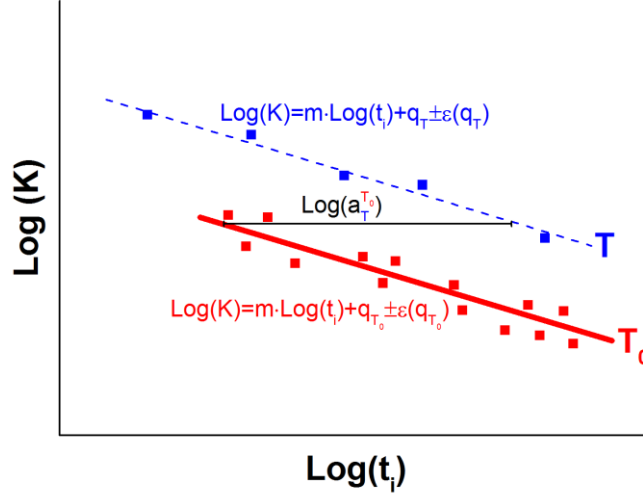

Figure 4 - Sketch of the procedure used for the evaluation of the shift factors and their errors.
ε represents the standard error.

Firstly, the temperature of 60°C (for which the greatest number of experimental points was available for the two materials) was considered as the reference temperature, T_0. $\log K$ vs. $\log t_i$ data were linearly fitted evaluating the slope m and the corresponding intercept q. The standard error $\varepsilon(m)$ was found to be negligible in comparison with $\varepsilon(q)$ which was calculated according to Equation 6:

$$\varepsilon(q) = s_\varepsilon \sqrt{\frac{\sum_{i=1}^{n}\left(\log t_{i,i}\right)^2}{n \cdot \sum_{i=1}^{n}\left(\log t_{i,i} - \log \bar{t}_i\right)^2}} \tag{6}$$

in which n is the number of experimental points, $\bar{t}_i$ is the average crack initiation time and s_ε is the standard deviation, evaluated according to Equation 7:

$$s_\varepsilon = \sqrt{\frac{\sum_{i=1}^{n}\left(\log K_i - \log \widehat{K}_i\right)^2}{n - 2}} \tag{7}$$

Here, $\log \widehat{K}_i$ is the value of the interpolating function for a given experimental datum i.

In accordance with the time-temperature equivalence postulate, the curves obtained at different temperatures were assumed to have the same shape and thus they were linearly fitted using the same slope m. The fit was reasonably good for all temperatures, denoting a power-law dependence of K vs. t_i. The shift factor, $\log a_T^{T_0}$, between any given curve at temperature T and the reference one at T_0 was then evaluated using Equation 8:

$$\log a_T^{T_0} = \frac{q_T - q_{T_0}}{m} \tag{8}$$

The absolute standard error, $\varepsilon_T^{T_0}$, related to the determination of $\log a_T^{T_0}$ can be defined as per Equation 9:

$$\varepsilon_T^{T_0} = \frac{\varepsilon(q_{T_0}) + \varepsilon(q_T)}{m} \qquad (9)$$

This slightly elaborated procedure was applied on the four separate datasets available for each material, corresponding to initiation/propagation in both environments (air and solutions). The reason for this lies in the limited range of temperatures investigated, especially compared to the relative high data scatter observed in fracture data. Unfortunately, temperatures above 60°C could not be considered because of solution evaporation and possible changes in its chemical activity. On the other end, tests at temperature below 40°C were highly time-consuming and for this reason just a few were run at 23 or 31°C, and only in air.
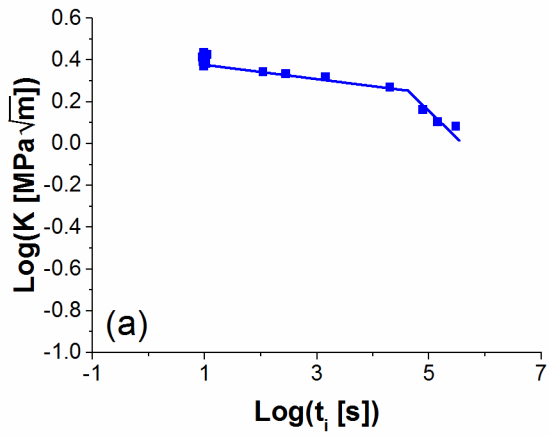
3   Results

The initiation ($\log K$ vs. $\log t_i$) and propagation ($\log K$ vs. $\log \dot{a}$) curves of the two materials are reported in Figures 5 to 8.

Considering first the in-air fracture initiation for the two materials at 23°C (filled symbols in Figure 5(a) and Figure 6(a)) a variation in the slope of the two curves, more pronounced in the case of HDPE-BI, can be observed at a value of K of about 2 MPa·m$^{1/2}$ (corresponding to $\log K = 0.3$). This variation, as confirmed by the fractographic analysis conducted in [24] and already reported in previous works [11, 31-33], can be attributed to a transition from a relatively ductile to a more brittle fracture behaviour. As reported in Figure 5(a,c,e) – for the temperatures in which both slopes are visible – the time at which this transition takes place decreases with increasing temperature, while no appreciable variation in the value of the corresponding stress intensity factor can be detected. In the case of HDPE-MONO only few data points are available in the region of $K > 2$ MPa·m$^{1/2}$ at high temperature and, as a consequence, this transition cannot be clearly observed in the available data. For what concerns the in-air propagation behaviour, as reported in Section 2.1, only data obtained from creep tests (which were conducted exclusively in the brittle region) are available.
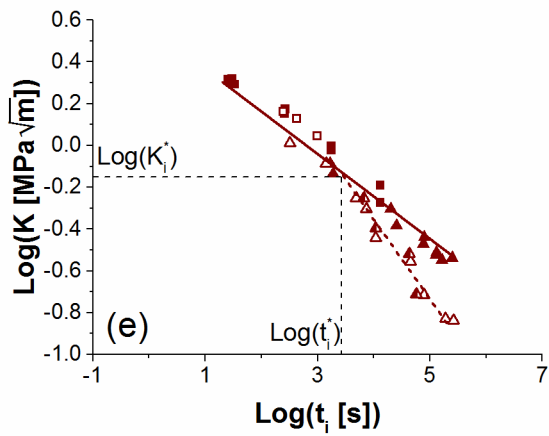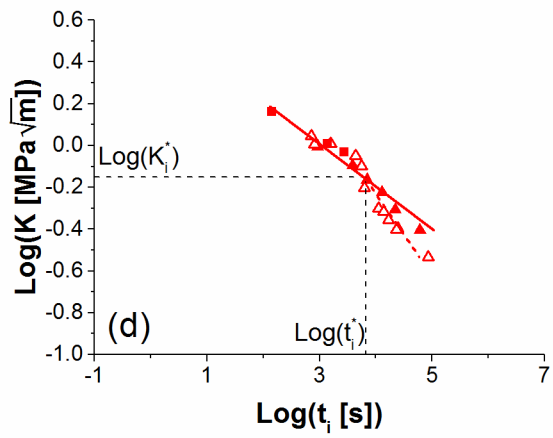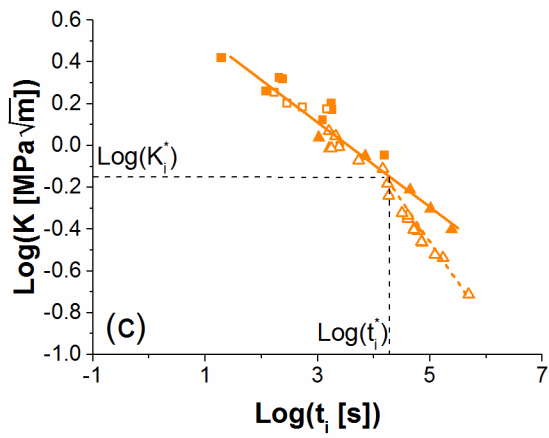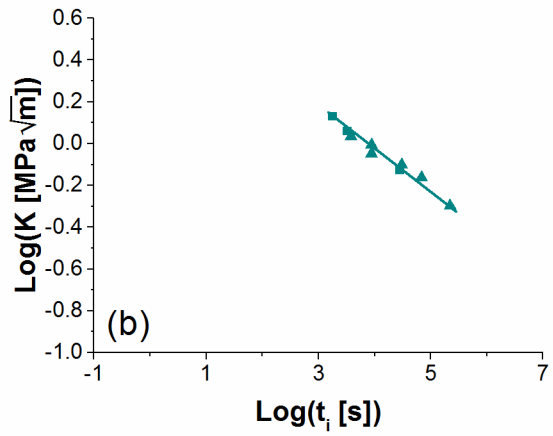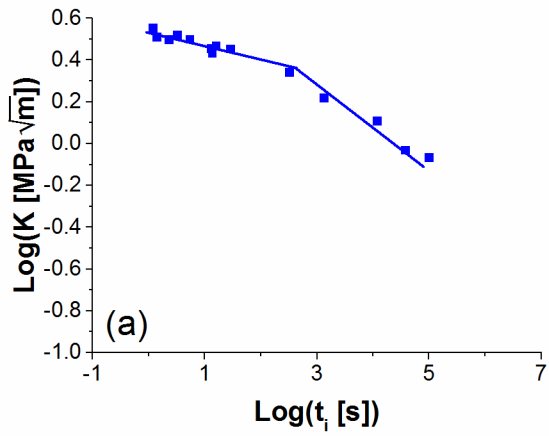
Data obtained in the two active environments (empty symbols in Figures 5-8) again confirm that Sol. A and B act as ESC agents for both materials and they have the same effect irrespective of the presence of sodium hypochlorite, as previously observed in [24]. From the intersection of the air and environment branches of the fracture curves (which always occur in the brittle region), several quantities can be defined: a critical interaction time t_i^*, a critical crack speed $\dot{a}^*$, and the relevant stress intensity factors, K_i^* and K_p^*, which coincide and for both materials are equal to 0.7 MPa·m$^{1/2}$ ($\log K^* = -0.15$). If fracture initiates before t_i^* or propagates faster than $\dot{a}^*$, there is no effect of the environment; otherwise, fracture toughness is reduced bringing an earlier initiation and a higher crack speed for a given stress intensity factor. Temperature shifts the values of t_i^* and $\dot{a}^*$ while the corresponding critical stress intensity factors seem to be independent of it.

Since temperature does not affect the critical values of K (in terms of neither environment interaction nor ductile-brittle transition) or the slope of the corresponding branches of the curves at different temperatures, time-temperature superposition seems to be applicable. Therefore, initiation and propagation master curves for the two materials can be constructed by applying a simple horizontal shift along the logarithmic time axis.

Figure 5 - Crack initiation behaviour of HDPE-BI at different temperatures: (a) 23°C, (b) 31°C, (c) 40°C, (d) 50°C, (e) 60°C. The ductile to brittle transition and the effect of the two environments can be observed in (a,c,e) and (c,d,e) respectively.

Figure 6 - Crack initiation behaviour of HDPE-MONO at different temperatures: (a) 23°C, (b) 31°C, (c) 40°C, (d) 50°C, (e) 60°C. The ductile to brittle transition and the effect of the two environments can be observed in (a) and (c,d,e) respectively.
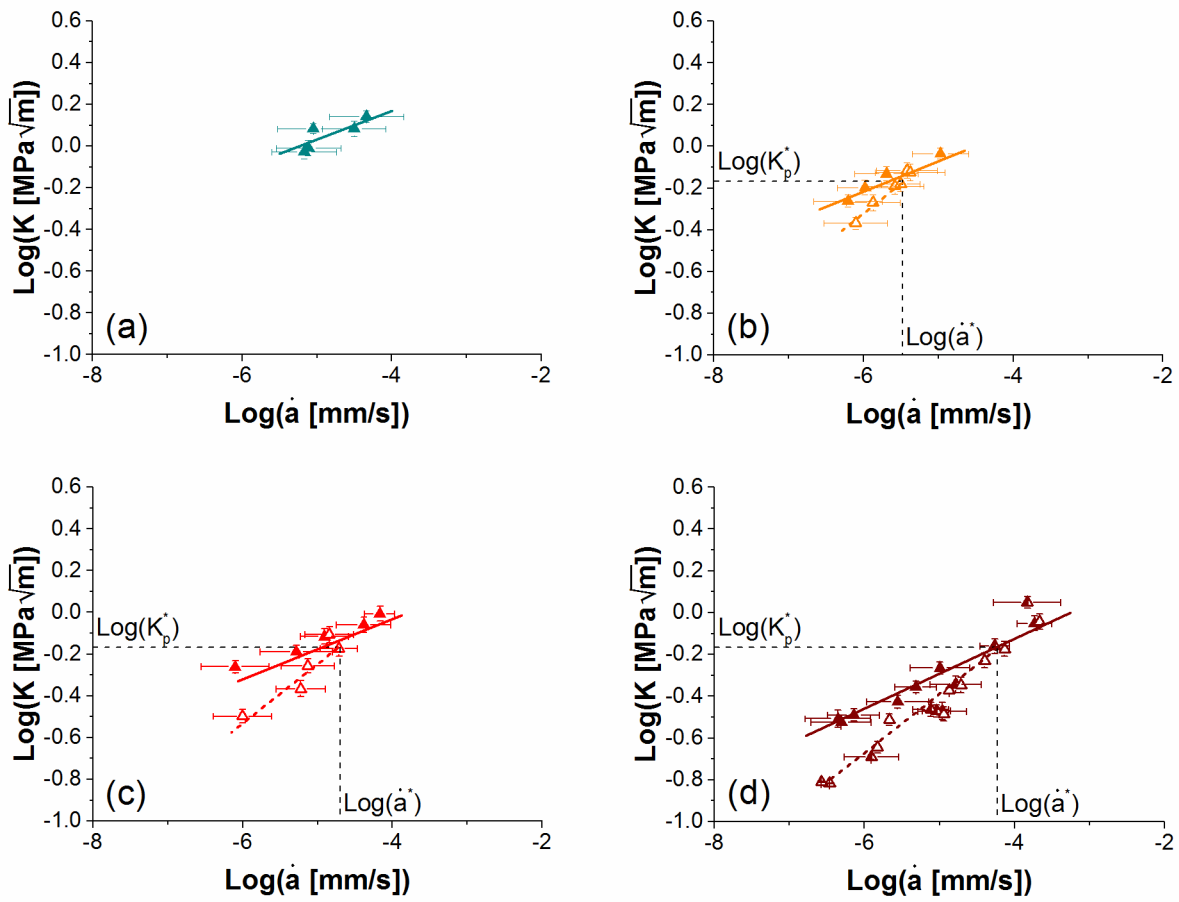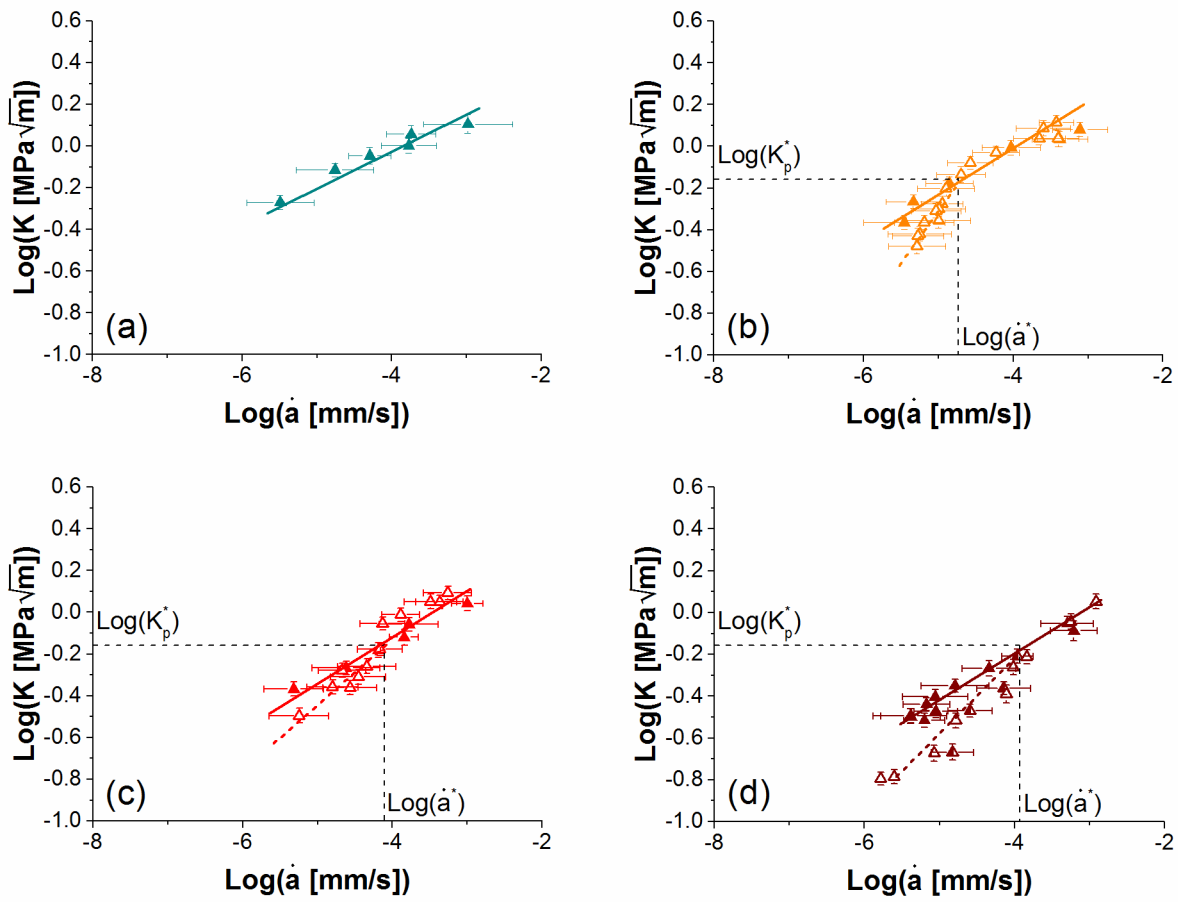
Figure 7 - Crack propagation behaviour for the HDPE-BI at different temperatures: (a) 31°C, (b) 40°C, (c) 50°C, (d) 60°C. The effect of the two environments can be observed in (b,c,d).

Figure 8 - Crack propagation behaviour for the HDPE-MONO at different temperatures: (a) 31°C, (b) 40°C, (c) 50°C, (d) 60°C. The effect of the two environments can be observed in (b,c,d).

The procedure described in Section 2.3.1 was hence applied to identify the shift factors, evaluating possible differences in the temperature dependence of the fracture behaviour in air and in the active environment. The brittle branch of the in-air curve was considered for the fitting; data obtained in the active environments below t_i^* and above $\dot{a}^*$ were considered together with in-air since no ESC occurs in these cases.

The four relevant shift factors obtained (initiation/propagation, in-air/environment) for both HDPE-BI and HDPE-MONO are plotted in Figure 9, where they can be seen to follow an Arrhenius law. While shift factors for the two polymers differ slightly, for each one the shift factors obtained separately on the four datasets show a good agreement, considering the uncertainty related to their evaluation. The agreement between initiation and propagation shift factors confirms the robustness of the method employed. For each material a single shift factor was thus obtained by fitting all the data on the relevant Arrhenius plot, represented by the continuous straight lines in Figure 9.
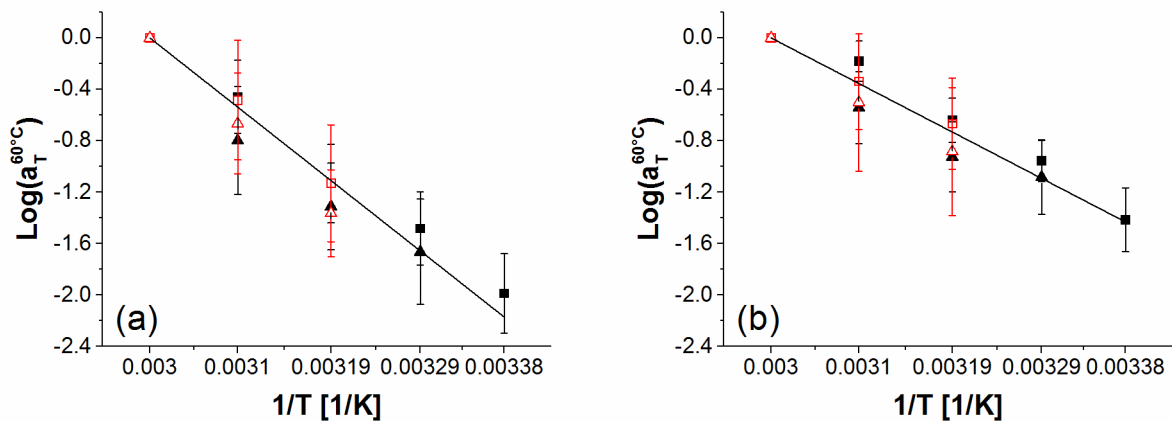
Figure 9 - Shift factors for HDPE-BI (a) and HDPE-MONO (b); T_0=60°C. Continuous lines represent a best fit of the concatenate set of data (initiation/propagation and air/environment) for each material.
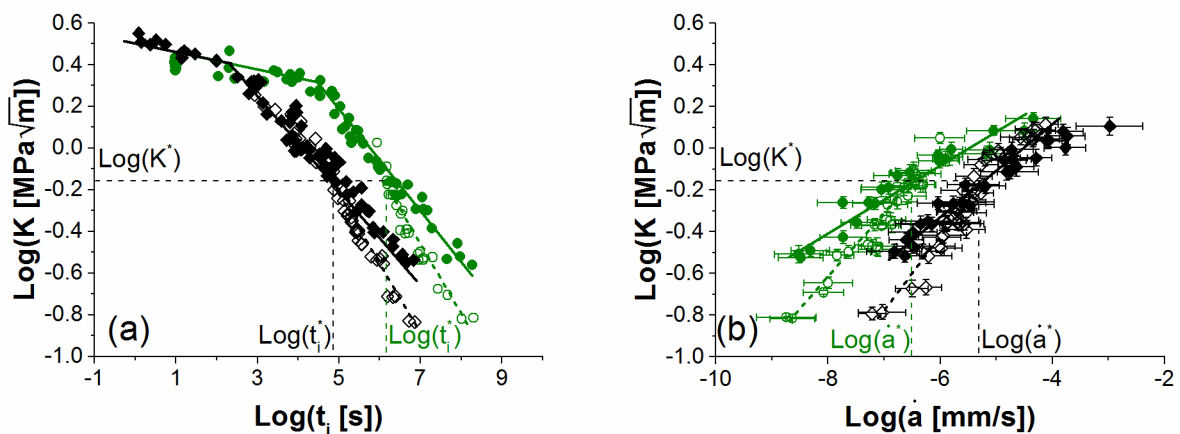
Figure 10 - Master curves of the two materials at 23°C. (a) initiation; (b) propagation.

Finally, the averaged shift factors were used to build fracture initiation ($\log K$ vs. $\log t_i$) and propagation ($\log K$ vs. $\log \dot{a}$) master curves for the two materials, displayed in Figure 10 at the reference temperature of 23°C.

4   Discussion

Time temperature superposition has been previously applied to fracture data [11, 27, 29, 30]. Nevertheless, it has to be noticed that coincidence between shift factors in air and in the active environment implies that, in the considered range of temperatures, the

solutions investigated (with our without sodium hypochlorite) do not influence the time-dependence of the fracture behaviour, which is determined only by the viscoelasticity of the two polymers and not by a change in aggressiveness of the solution with temperature.

Furthermore, since a simple horizontal shift is sufficient to overlap data both in-air and in the active environment, a single critical interaction stress intensity factor, K^*, can be found which does not depend on temperature. This means that it is the magnitude of the applied K that determines whether ESC occurs or not and temperature determines only the time necessary for ESC to occur.

From a design perspective, it is possible to determine a critical time to failure (which is the sum of initiation and propagation times) for a given product with a known initial defect size; this time is determined by t_i^* and $\dot{a}^*$. If the expected lifetime of the product is shorter than this critical value, ESC won't occur and the fracture behaviour will not be affected by the environment. For longer lifetimes, the effect of the active environment must be considered. This critical interaction time decreases with increasing temperature according to time-temperature equivalence.

Finally, the fracture behaviour of the two polyethylenes considered in this work can be compared. A first observation is that the master curves for HDPE-MONO and HDPE-BI have essentially the same shape, and in particular they display identical slopes in all three branches (ductile, brittle-air and brittle-environment). The main difference is that for HDPE-MONO the ductile-brittle transition occurs at shorter times: this result was expected, since HDPE-BI possesses a significantly larger fraction of long polymeric chains. As reported in [31], in fact, the brittle failure of a semicrystalline polymer is related to fracture of the so-called tie-molecules, connecting the various crystalline lamellae. At relatively low level of applied stress (in the brittle failure region), tie-molecules have time to untangle while relaxing and they can reach their full extension before failure. In the case of HDPE-BI, a longer time is required for this phenomenon to occur because of the high length tail in the molecular weight distribution. At higher stress instead, fracture occurs before the tie molecules can disentangle; since at the time of failure a great number of them is still acting as a bridge between the crystalline domains, the lamellae break up in "mosaic blocks" generating the typical rough fracture surface observed for ductile failure, as reported in [24] for the same two materials. In this regime, the difference in MWD does not play an important role and the response is governed by the crystalline phase, whose fraction is approximately the same for the two materials under study.

The equality between the slopes of the $\log K$ vs. $\log t_i$ and $\log K$ vs. $\log \dot{a}$ curves in the environment (and consequently of the critical stress intensity factor K^*) for HDPE-MONO and HDPE-BI, suggests that the same fracture mechanism occurs during failure of the two materials in presence of the active solutions. The accelerating effect of the ESC agent can be linked to a faster disentanglement rate of the tie molecules in the brittle regime [9, 10, 34] although localized chemical aging at the crack tip [35] cannot be excluded.

5   Conclusions

Slow crack growth and environmental stress cracking resistance of two HDPEs used for the manufacturing of bleach bottles were assessed, at different temperatures, using a LEFM approach. Time-temperature equivalence was successfully applied to fracture data.

The master curves in air have the same shape with a ductile to brittle transition observed for both materials. Its onset for the bimodal HDPE was delayed with respect to the monomodal grade as expected from the different molecular weight distribution of the two polymers.

In the presence of the two active environments (bleach solutions with and without sodium hypochlorite), below a critical value of the stress intensity factor K^*, the two materials displayed shorter initiation times and faster crack propagation rates. No difference in the effect of the two solutions was detected, confirming that, as previously reported in [24], sodium hypochlorite does not influence the ESC resistance of HDPE. This conclusion is valid when, as it is the case for commercial bleach solutions, a high pH prevents the dissociation of the chemical constituents to give active chlorine. Presence of the latter could give rise to local degradation at the crack tip with would further reduce fracture resistance with respect to the pure ESC case.

The curves describing initiation and propagation behaviour in the active environment at different temperatures can be superimposed using the same shift factor found in air. Critical interaction times and critical crack speeds, below and above which there is no effect of the environment, were identified for both polymers; they all correspond to the same K^*, irrespective of testing temperature.

These results are an indication of the fact that, in the considered range, the aggressiveness of the active environment is not altered by the temperature which only acts by accelerating or decelerating the fracture process according to the material inherent viscoelasticity. In particular, ESC occurs in the brittle failure regime which is most likely dominated by the disentanglement of the tie molecules and this process is favoured by the ESC agents.

The applicability of time-temperature equivalence also in the case of ESC is very important: this result can lead to the use of fracture mechanics data, obtained from temperature accelerated tests, for the prediction of the long-term behaviour of polymeric products also in presence of aggressive environments. Of course, its validity needs to be demonstrated for other cases involving different systems (polymer+environment).

6   Acknowledgements

7   References

[1]   J. A. Jansen, "Environmental stress cracking. The plastic killer," Advanced Materials & Processes, vol. 162, no. 7, pp. 50-3, 2004.

[2]   T. Nielsen and C. Hansen, "Surface wetting and the prediction of environmental stress cracking (ESC) in polymers," *Polymer Degradation and Stability,* vol. 89, pp. 513-16, 2005.

[3]   C. Hansen, "On predicting environmental stress cracking in polymers," *Polym Degrad Stab,* vol. 77, pp. 43-53, 2002.

[4]   M. Munaro and L. Akcelrud, "Polyethylene blends: A correlation study between morphology and environmental resistance," *Polymer Degradation and Stability,* vol. 93, no. 1, pp. 43-9, 2008.

[5]   Y. Men, J. Rieger, H. Enderle and D. Lilge, "The mobility of the amorphous phase in polyethylene as a determining factor for slow crack growth," *The European Physical Journal E,* vol. 15, no. 4, pp. 421-5, 2004.

[6]   A. Sharif, N. Mohammadi and S. Ghaffarian, "Practical Work of Crack Growth and Environmental Stress Cracking Resistance of Semicrystalline Polymers," *Journal of Applied Polymer Science,* vol. 110, pp. 2756-62, 2008.

[7]   N. Brown, X. Lu, Y-L. Huang and R. Qian, "Slow crack growth in polyethylene – a review", *Macromolecular Symposia*, vol. 41, pp. 55-67, 1991.

[8]   J. Cazenave, R. Seguela, B. Sixou and Y. Germain, "Short-term mechanical and structural approaches for the evaluation of polyethylene stress crack resistance," *Polymer,* vol. 47, pp. 3904-14, 2006.

[9]   L. Kurelec, M. Teeuwen, H. Schoffeleers and R. Deblieck, "Strain hardening modulus as a measure of environmental stress crack resistance of high density polyethylene," *Polymer,* vol. 46, pp. 6369-79, 2005.

[10]   M. Fleissner, "Experience with a full notch creep test in determining the stress crack performance of polyethylenes," *Polymer Engineering and Science,* vol. 38, no. 2, pp. 330-40, 1998.

[11]   L. Andena, M. Rink, R. Frassine and R. Corrieri, "A fracture mechanics approach for the prediction of the failure time of polybutene pipes," *Engineering Fracture Mechanics,* vol. 76, pp. 2666-77, 2009.

[12]   P. Hutař, M. Ševčík, A. Frank, L. Náhlík, J. Kučera and G. Pinter, "The effect of residual stress on polymer pipe lifetime," *Engineering Fracture Mechanics,* vol. 108, pp. 98-108, 2013.

[13]   A. Frank, W. Freimann, G. Pinter and R. Lang, "A fracture mechanics concept for the accelerated characterization of creep crack growth in PE-HD pipe grades," *Engineering Fracture Mechanics,* vol. 76, pp. 2780-87, 2009.

[14]   P. Hutař, M. Ševčík, L. Náhlík, G. Pinter, A. Frank and I. Mitev, "A numerical methodology for lifetime estimation of HDPE pressure pipes," *Engineering Fracture Mechanics,* vol. 78, pp. 3049-58, 2011.

[15]   J. Williams and G. Marshall, "Environmental Crack and Craze Growth Phenomena in Polymers," *Proceedings of the Royal Society A, Mathematical Physical and Engineering Sciences,* vol. 342, pp. 55-77, 1975.

[16]   M. A. Kamaludin, Y. Patel, J. G. Williams and B. R. Blackman, "A fracture mechanics approach to characterising the environmental stress cracking behaviour of thermoplastics," *Theoretical and Applied Fracture Mechanics,* vol. 92, pp.373-80, 2017.

[17]   L. Andena, L. Castellani, A. Castiglioni, A. Mendogni, M. Rink and F. Sacchetti, "Determination of environmental stress cracking resistance of polymers: Effects of loading history and testing configuration," *Engineering Fracture Mechanics,* vol. 101, pp. 33-46, 2013.

[18]   L. Andena, M. Rink, C. Marano, F. Briatico-Vangosa and L. Castellani, "Effect of processing on the environmental stress cracking resistance of high-impact polystyrene," *Polymer Testing,* vol. 54, pp. 40-7, 2016.

[19]   V. Alstaedt, S. Keiter, M. Renner and A. Schlarb, "Environmental Stress Cracking of Polymers Monitored by Fatigue Crack Growth Experiments," *Macromolecular Symposia,* vol. 214, pp. 31-46, 2004.

[20]   M. Rink, R. Frassine, P. Mariani and G. Carianni, "Effects of detergent on crack initiation and propagation in polyethylenes," *Fracture of Polymers, Composites and Adhesives II,* vol. 32, pp. 103-14, 2003.

[21]   L. Andena, L. Castellani, L. Franchini, J. Menegari, M. Rink and F. Sacchetti, "Environmental crack initiation and propagation in polyethylene under different loading conditions," in *DYFP2012: Proceedings of the 15th International Conference on Deformation, Yield and Fracture of Polymers*, Rolduc Abbey, Kerkrade, the Netherlands, McKenna G., Govaert L., 1-5 April 2012, pp. 182-5.

[22]   M. A. Kamaludin, Y. Patel, B. Blackman and J. G. Williams, "Fracture mechanics testing for environmental stress cracking in thermoplastics," *Procedia Structural Integrity,* vol. 2, pp. 227-34, 2016.

[23]   E. J. Moskala, "A fracture mechanics approach to environmental stress cracking in poly(ethyleneterephthalate)," *Polymer,* vol. 39, pp. 675-80, 1998.

[24]   M. Contino, A. Colombo, L. Andena, M. Rink and G. Marra, "Fracture of high-density polyethylene for bleach bottles," *Procedia Structural Integrity,* vol. 2, pp. 213-20, 2016.

[25]   T. L. Anderson, Fracture Mechanics. Fundamentals and Applications, Boca Raton (Florida,U.S.A.): CRC press, 1995.

[26]   D. P. Rooke and D. J. Cartwright, Compendium of stress intensity factors, Uxbridge (Middlesex,U.K.): The Hillingdon Press, 1976.

[27]   R. Frassine, M. Rink, A. Leggio and A. Pavan, "Experimental analysis of viscoelastic criteria for crack initiation and growth in polymers," *International Journal of Fracture,* vol. 81, pp. 55-75, 1996.

[28]   P. Mariani, R. Frassine, M. Rink and A. Pavan, "Viscoelasticity of Rubber-Toughened Poly(Methyl Methacrylate). Part I: Deformational Behavior," *Polymer Engineering and Science,* vol. 36, no. 22, pp. 2750-7, 1996.

[29]   P. Mariani, R. Frassine, M. Rink and A. Pavan, "Viscoelasticity of Rubber-Toughened Poly(Methyl Methacrylate). Part II: Fracture Behavior," *Polymer Engineering and Science,* vol. 36, no. 22, pp. 2758-64, 1996.

[30]   T. Pini, F. Briatico-Vangosa, R. Frassine and M. Rink, "Fracture toughness of acrylic resins: viscoelastic effects and deformation mechanisms," *Polymer Engineering Science,* vol. 58, no.3, pp. 369-76, 2017.

[31]   A. Lustiger, "Environmental Stress Cracking: The Phenomenon and Its Utility," in *Failure of Plastics*, Munich, Vienna, New York, Hanser Publishers, pp. 305-29, 1986.

[32]   R. K. Krishnaswamy, "Analysis of ductile and brittle failures from creep rupture testing of high-density polyethylene (HDPE) pipes," *Polymer,* vol. 46, pp. 11664-72, 2005.

[33]   R. A. Deblieck, D. Van Beek, K. Remerie and I. M. Ward, "Failure mechanisms in polyolefines: The role of crazing, shear yielding and the entanglement network," *Polymer,* vol. 52, pp. 2979-90, 2011.

[34]   A. Y. Yarysheva, E. G. Rukhlya, L. M. Yarysheva, D. V. Bagrov, A. L. Volynskii, N. F. Bakeev, "The structural evolution of high-density polyethylene during crazing in liquid medium, " *European Polymer Journal, vol.* 66, pp. 458–69, 2015.

[35]   G. Pinter, M. Haager, C. Wolf, R. W. Lang, "Thermo-Oxidative Degradation during Creep Crack Growth of PE-HD Grades as Assessed by FT-IR Spectroscopy," *Macromolecular Symposia, vol. 217, pp. 307-16, 2004.*